SUPPORTING INFORMATION

Conjunction of Chirality and Slow Magnetic Relaxation in the Supramolecular Network Constructed of Crossed Cyano-Bridged Co^{II}-W^{V} Molecular Chains

Szymon Chorazy,[†,‡] Koji Nakabayashi,[‡] Kenta Imoto,[‡] Jacek Mlynarski,[†] Barbara Sieklucka,[†,*] and Shin-ichi Ohkoshi[‡,#,*]

[†]Faculty of Chemistry, Jagiellonian University, Ingardena 3, 30-060 Cracow, Poland, [‡]Department of Chemistry, School of Science, The University of Tokyo, 7-3-1 Hongo, Bunkyo-ku, Tokyo, 113-0033, Japan, and [#]CREST, JST, K's Gobancho, 7 Gobancho, Chidoya-ku, Tokyo, 102-0076, Japan

1. The design of coordination polymers **1**-(*SS*) and **1**-*(RR)*

The octacyanotungstate(V) ions with 3d divalent metal centers in simple alcohol solutions forms 0D $\{M^{II}[M^{II}(solv)_3]_8[W^V(CN)_8]_6 \cdot n(solv)\}_m$ (M=Mn, Co, Ni; solv=MeOH, EtOH) clusters of a six-capped body-centered cube topology (scheme 1).[S1-S3] In these molecules each external M^{II} center forms three cyanide bridges with W^V. Three remaining positions of these ions are occupied by faciale arranged solvent molecules which can be easily substitute by other organic ligands. This synthetic strategy leads to surface modification of clusters by bidentate capping ligands[S4-S6] or to the formation of coordination networks with $M^{II}_9W^V_6$ molecules as secondary building units in the case of using organic spacers (scheme 1).[S7-S8] Original clusters as well as the most of their derivatives exhibit large structural rearrangement during exposition to the air due to the fast exchange of coordinated and crystallization alcohol molecules by water. Unfortunately this process is rather uncontrolled and leads to multi-phase or amorphous material.[S8] The possible reason is the presence of very labile solvent molecules in the crystal structure or/and instability of the cluster core in contact with water. The observed MeOH to H_2O exchange process is related not only for crystallization but also to coordinated solvent molecules changing the coordination spheres of magnetically active 3d metal ions. To induce that in controlled manner, we applied rigid tridentate *i*Pr-Pybox ligand with the strong preference to form *mer* configuration which hinders the growth of 0D clusters and extorts 1D molecular architecture and crossed arrangement of chains in the same synthetic conditions as for clusters. It is worth noting that synthetic solution prepared by dissolving of cobalt(II) chloride, sodium octacyanotungstate(V) and iPr-Pybox in methanol is very stable and nothing crystallizes for months. This is in the great contrast with the similar solution *without* organic ligand from which 0D $Co^{II}_9W^V_6$ clusters growths very quickly which shows the strong competition between synthetic paths leading to clusters and to higher dimensional assemblies. Exclusively the addition of non-polar diisopropyl ether disturbs the metastable equilibrium and allows the crystallization of **1**-(S*S*) and **1**-(*RR*). The same type of polymer was obtained by Li et al.[S9] by precipitation of polycrystal powder in MeOH and later dissolving resultant solid in dimethylformamide but for that case chains:

1) are typically arranged parallel without microporous character
2) crystallize in centrosymmetric $P\bar{1}$ space group
3) are not well magnetically isolated as long-range magnetic ordering below 10K is observed.

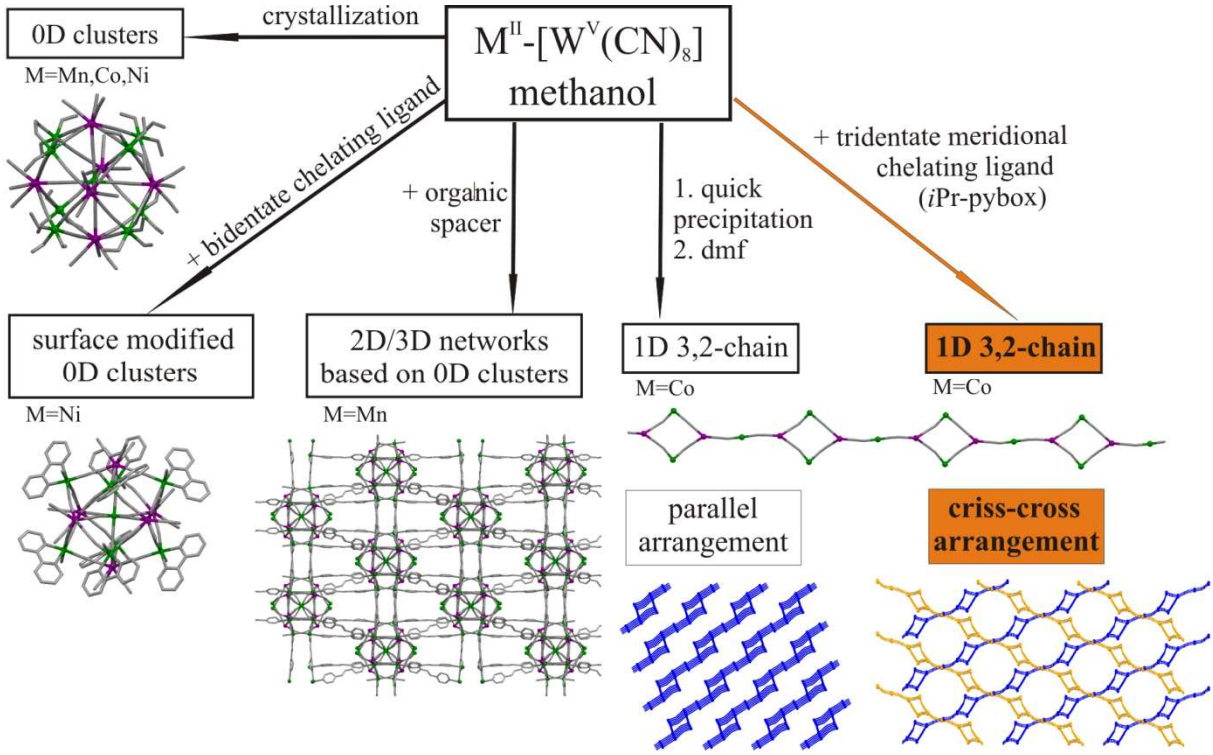

Scheme 1 Coordination compounds based on 3d metal ions and octacyanotungstate(V) obtained in methanolic solution. Orange colour shows synthetic route described in this paper.

2. Experimental details

2a. Materials

Chemicals and solvents used in the syntheses were purchased from commercial sources (Tokyo Chemical Industry, Wako Chemicals GmbH) and used without further purification. $Na_3[W(CN)_8]\cdot 4H_2O$ was synthesized according to the published procedure.[S10]

2b. Synthesis of {[Co^{II}(*SS*-*i*Pr-Pybox)(MeOH)]$_3$[$W^V(CN)_8$]$_2\cdot$6MeOH}$_n$ **1**-(*SS*)

(*SS*)-*i*Pr-Pybox (0.06mmol, 18.1mg) dissolved in 4.0 mL of methanol was added to a freshly prepared methanolic solution (6.0 mL) of $CoCl_2\cdot 6H_2O$ (0.06mmol, 14.3mg) and $Na_3[W(CN)_8]\cdot 4H_2O$ (0.04mmol, 21.3mg). To resultant orange solution 5.0 mL of diisopropyl ether was added with gentle stirring. This gave an orange suspension which was left to stand in the dark. Well-shaped orange rhombic platelet crystals of **1**-(*SS*) were observed after five days. Yield 28 mg, 66%. The composition of **1**-(*SS*) was established from results of X-ray diffraction measurements. IR (in Apiezon® N, cm^{-1}): 2180m, 2173m, 2160m, 2148m, 2142m, ν(C≡N). Only the range of CN^- stretching vibrations (2300-1900 cm^{-1}) was interpreted due to large variable background of Apiezon® N for lower and higher frequencies. Obtained material is stable in the mother liquid and diisopropyl ether solution as well as in Apiezon® N grease. During drying on the air the phase transition to hydrated phase, **1**-(*SS*)-**hyd** is observed. The formula of air stable **1**-(*SS*)-**hyd** is {[Co^{II}(*SS*-*i*Pr-Pybox) $(H_2O)]_3[W^V(CN)_8]_2\cdot 7H_2O\}_n$ as was determined from inductively coupled plasma mass spectroscopy (Co, W) and standard microanalytical methods (C, H, N). Calcd. for $Co_3W_2C_{67}H_{89}N_{25}O_{16}$: Co, 8.65%; W, 17.98%; C, 39.35%; H, 4.39%; 17.12%. Found: Co, 8.74%; W, 18.14%; C, 39.09%; H, 4.45%; N, 16.96%. The yield and the amount of magnetically active sample for magnetic measurements were calculated based on the mass of **1**-(*SS*)-**hyd** and the effective decrease in molar mass on going from **1**-(*SS*) to **1**-(*SS*)-**hyd.**

2c. Synthesis of {[Co^{II}(*RR*-*i*Pr-Pybox)(MeOH)]$_3$[$W^V(CN)_8$]$_2\cdot$6MeOH}$_n$ **1**-(*RR*)

The analogous procedure to that used for (*SS*)-*i*Pr-Pybox enantiomorph was employed. Orange rhombic platelet crystals of **1**-(*RR*) appeared after five days. Yield 26 mg, 59%. IR (Apiezon® N): 2181m, 2171m, 2160m, 2148m, 2142m, ν(C≡N). The stability of **1**-(*RR*) is similar to that observed for **1**-(*SS*) and during exposition to the air **1**-(*RR*) undergoes the transformation into hydrated phase, **1**-(*RR*)-**hyd.** The formula of air-stable **1**-(*RR*)-**hyd** is {[Co^{II}(*RR*-*i*Pr-Pybox) $(H_2O)]_3[W^V(CN)_8]_2\cdot 7H_2O\}_n$. Anal. (ICP-MS, CHN analysis). Calcd. for $Co_3W_2C_{67}H_{89}N_{25}O_{16}$:

Co, 8.65%; W, 17.98%; C, 39.35%; H, 4.39%; 17.12%. Found: Co, 8.61%; W, 17.96%; C, 39.14%; H, 4.44%; N, 17.05%.

2d. Crystal Structure Determination

Single crystal diffraction data of **1**-(*SS*) and **1**-(*RR*) were collected on a Rigaku R-AXIS RAPID imaging plate area detector with graphite monochromated Mo Kα radiation. The single crystals were dispersed in Apiezon® N, mounted on Micro Mounts™ and measured at 90(2)K. The crystal structures were solved by a direct method and refined by a full-matrix least-squares technique using SHELXL-97.[S11] All calculations were performed using the Crystal Structure crystallographic software package. All non-hydrogen atoms were refined anisotropically while the hydrogen atoms were refined using the riding model. The most of solvent molecules were structurally disordered and therefore two crystallographic positions for some of atoms were proposed. Structural diagrams were prepared using Mercury 1.2.3. software. CCDC reference numbers 893866 (**1**-(*SS*)) and 893867 (**1**-(*RR*)).

2e. Physical Techniques

Elemental analyses of Co and W for the powder samples were measured by Agilent 7700 Series inductively coupled plasma mass spectrometer (ICP-MS), while those of C, H, N were determined by standard microanalytical methods. IR spectra were recorded on JASCO FTIR-4100 spectrometer in the 4000-400 cm^{-1} range with the CaF_2 plates on crystals dispersed in Apiezon® N. The magnetic properties were measured by a superconducting quantum interference device (SQUID) magnetometer (Quantum Design, MPMS 7) in the 2-300K range. To prevent solvent exchange the samples of **1**-(*SS*) and **1**-(*RR*) were measured being closed with the mother liquid in a glass tube. Single crystal magnetic study of **1**-(*SS*) was carried out on the chosen fully-developed crystal covered by Apiezon® N and mounted on the rotator. Diamagnetic corrections for all magnetic signals were subtracted. The UV-Vis diffuse reflectance spectra were measured by a Shimadzu UV-3100 spectrometer with CaF_2 plates on the powder samples dispersed in Apiezon® N and corrected by the background coming from Apiezon grease. The NCD spectra were recorded by JASCO E-250 spectrometer and the sample was prepared in the same way as for absorption spectra.

2f. Calculations

Continuous Shape Measure Analysis for coordination spheres of eight-coordinated W(V) ions for all phases was performed by SHAPE software ver. 1.1b.[S12-S14]

Table S1. Crystal Data and Structure Refinement for **1**-(*SS*) and **1**-(*RR*)

compound		**1**-(*SS*)	**1**-(*RR*)
method		single-crystal XRD	single-crystal XRD
formula		$Co_3W_2C_{75.5}N_{25}O_{15}H_{75.5}$	$Co_3W_2C_{75.5}N_{25}O_{15}H_{74}$
formula weight [g·mol^{-1}]		2117.59	2116.07
T [K]		90(2)	90(2)
λ [Å]		0.71075 (Mo Kα)	0.71075 (Mo Kα)
crystal system		monoclinic	monoclinic
space group		*C*2	*C*2
unit cell	***a* [Å]**	33.6487(7)	33.6237(8)
	***b* [Å]**	15.2675(3)	15.2570(4)
	***c* [Å]**	20.9931(4)	21.0243(6)
	β [deg]	119.3160(10)	119.3170(7)
V [Å^3]		9403.6(3)	9404.1(4)
Z		2	2
calculated density [g·cm^{-3}]		1.497	1.507
absorption coefficient [cm^{-1}]		3.025	3.026
F(000)		4216	4244
crystal size [mm x mm x mm]		0.30 x 0.15 x 0.10	0.25 x 0.15 x 0.05
Θ range [deg]		3.01 – 27.47	3.01 – 27.47
limiting indices		-39 < h < 43 -19 < k <19 -27 < l < 27	-42 < h < 43 -19 < k <19 -27 < l < 27
collected reflections		46582	72723
unique reflections		21288	21338
R_{int}		0.0631	0.0994
number of points		-	-
completeness [%]		99.6	99.4
max and min transmission		0.7518 and 0.4638	0.860 and 0.587
refinement method		full-matrix least-squares on F^2	full-matrix least-squares on F^2
data/restraints/parameters		21288/60/1114	21338/80/1132
Flack parameter		0.008(6)	0.007(6)
GOF on F^2		1.074	1.023
final *R* indices		R_1 = 0.0444 [$I > 2\sigma(I)$] wR_2 = 0.0888 (all data)	R_1 = 0.0493 [$I > 2\sigma(I)$] wR_2 = 0.1022 (all data)
largest diff peak and hole		1.470 and -2.118 e·A^{-3}	1.898 and -3.113 e·A^{-3}

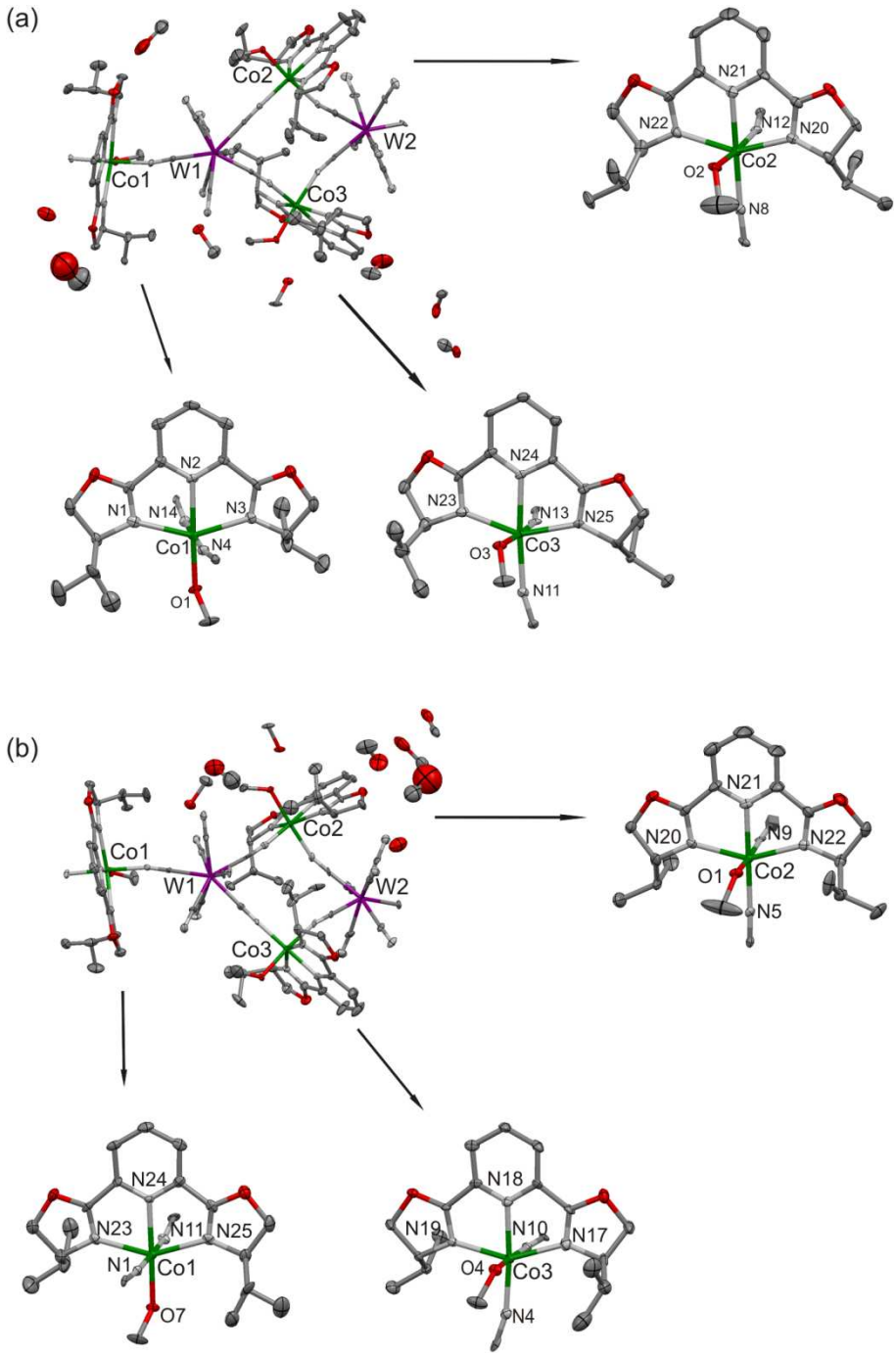

Figure S1. The crystal structure of **1**-(*SS*) (a) and **1**-(*RR*) (b): the asymmetric units with detailed description of Co(II) moieties. Atom spheres are shown with 40% probability ellipsoids. Hydrogen atoms are omitted for clarity. Colour code: W – purple, Co – green, O – red, C – dark grey, N – light grey. The part of methanol molecules is strongly disordered and they are presented in one of two possible crystallographic position.

Table S2. (part 1) Detailed structure parameters of **1**-(*SS*) and **1**-(*RR*)

Parameter	**1**-(*SS*)	**1**-(*RR*)
W1-C	2.144(7) - 2.186(6) Å	2.134(8) - 2.198(8) Å
W2-C	2.140(7) - 2.168(7) Å	2.134(8) - 2.170(11) Å
C-N (W1)	1.149(7) - 1.167(8) Å	1.133(11) - 1.182(2) Å
C-N (W2)	1.143(8) - 1.170(7) Å	1.141(13) - 1.170(2) Å
W1-C-N	173.6(5) - 179.4(8)°	173.0(6) - 179.1(8) Å
W2-C-N	172.6(6) - 179.0(5)°	172.5(6) - 179.8(8) Å
Co1-W1	5.352 Å	5.348 Å
Co1-W2	5.168 Å	5.166 Å
Co2-W1	5.398 Å	5.395 Å
Co2-W2	5.337 Å	5.337 Å
Co3-W1	5.294 Å	5.294 Å
Co3-W2	5.297 Å	5.294 Å
Co1-N-C	167.6(5)° (N4-C4) 149.6(5)° (N14-C14)	168.8(6)° (N1-C1) 150.6(6)° (N11-C11)
Co2-N-C	177.2(6)° (N8-C8) 163.8(6)° (N12-C12)	177.7(6)° (N5-C5) 164.1(7)° (N9-C9)
Co3-N-C	163.8(5)° (N11-C11) 163.7(5)° (N13-C13)	164.7(6)° (N4-C4) 162.3(7)° (N10-C10)
Co1-N(CN)	2.082(5) Å 2.091(5) Å	2.086(7) Å 2.089(7) Å
Co1-N(py)	2.102(5) Å	2.109(8) Å
Co1-N(ox)	2.169(6) Å 2.214(6) Å	2.158(8) Å 2.220(7) Å
Co1-O	2.033(4) Å	2.042(6) Å
(CN)N-Co1-N(CN)	177.8(2)°	178.0(3)°
(CN)N-Co1-O	91.80(19)° 87.22(19)°	91.9(3)° 87.7(3)°
(py)N-Co1-O	175.9(2)°	175.9(3)°
(py)N-Co1-N(CN)	89.2(2)° 91.8(2)°	88.7(3)° 91.7(3)°
(ox)N-Co1-N(ox)	149.0(2)°	149.0(3)°
(ox)N-Co1-N(py)	74.3(2)° 74.6(2)°	74.1(3)° 74.9(3)°
ox(N)-Co1-O	103.86(19)° 107.15(19)°	104.1(3)° 106.9(3)°
ox(N)-Co1-N(CN)	85.57(19)° 87.4(2)° 92.75(19)° 94.76(19)°	85.5(3)° 87.0(3)° 92.7(3)° 95.0(3)°

Table S2. (part 2) Detailed structure parameters of **1**-(*SS*) and **1**-(*RR*)

Parameter	**1**-(*SS*)	**1**-(*RR*)
Co2-N(CN)	2.063(6) Å 2.090(5) Å	2.060(7) Å 2.080(8) Å
Co2-N(py)	2.096(5) Å	2.104(7) Å
Co2-N(ox)	2.176(6) Å 2.199(6) Å	2.172(6) Å 2.195(7) Å
Co2-O	2.115(4) Å	2.118(8) Å
(CN)N-Co2-N(CN)	93.6(2)°	93.7(3)°
(CN)N-Co2-O	91.45(18)° 174.9(2)°	91.4(3)° 174.9(3)°
(CN)N-Co2-N(py)	86.5(2)° 179.7(2)°	86.3(3)° 179.7(3)°
(py)N-Co2-O	88.47(18)°	88.6(3)°
(ox)N-Co2-N(ox)	150.4(2)°	150.3(3)°
(ox)N-Co2-N(CN)	87.18(19)° 91.55(19)° 104.2(2)° 105.4(2)°	87.6(3)° 92.0(3)° 104.3(3)° 105.4(3)°
(ox)N-Co2-N(py)	74.8(2)° 75.5(2)°	74.9(3)° 75.4(3)°
(ox)N-Co2-O	87.50(18)° 91.19(18)°	86.8(3)° 91.0(3)°
Co3-N(CN)	2.060(5) Å 2.071(6) Å	2.053(10) Å 2.068(8) Å
Co3-N(py)	2.108(5) Å	2.105(10) Å
Co3-N(ox)	2.189(6) Å 2.191(6) Å	2.179(6) Å 2.194(7) Å
Co3-O	2.087(4) Å	2.085(6) Å
(CN)N-Co3-N(CN)	89.54(19)°	89.4(4)°
(CN)N-Co3-O	91.15(17)° 175.5(2)°	91.3(3)° 175.8(3)°
(CN)N-Co3-N(py)	91.20(19)° 175.0(2)°	91.4(4)° 175.2(3)°
(py)N-Co3-O	88.50(18)°	88.3(3)°
(ox)N-Co3-N(ox)	150.27(18)°	150.1(4)°
(ox)N-Co3-N(CN)	84.9(2)° 92.1(2)° 99.7(2)° 109.8(2)°	85.3(3)° 91.4(4)° 99.4(3)° 110.3(3)°
(ox)N-Co3-N(py)	75.2(2)° 75.3(2)°	74.5(3)° 75.8(3)°
(ox)N-Co3-O	90.62(19)° 92.16(19)°	90.6(3)° 92.6(2)°

Table S3 Results of Continuous Shape Measure analysis for $[W^{V}(CN)_8]^{3-}$ units in **1**-(*SS*) and **1**-(*RR*)

$[W1(CN)_8]^{3-}$ in	**1**-(*SS*)	**1**-(*RR*)
CSM BTP-8	1.745	1.732
CSM SAPR-8	0.753	0.776
CSM DD-8	0.870	0.850
$[W2(CN)_8]^{3-}$ in	**1**-(*SS*)	**1**-(*RR*)
CSM BTP-8	1.475	1.510
CSM SAPR-8	0.570	0.545
CSM DD-8	1.222	1.223

Legend: CSM BTP-8 – the shape measure parameter relative to the bicapped trigonal prism; CSM SAPR-8 – the shape measure parameter relative to the square antiprism; CSM DD-8 – the shape measure parameter relative to the dodecahedron (triangular dodecahedron); CSM = 0 for the ideal geometry and increases with the degree of distortion.

Table S4 Ideal and observed dihedral δ and φ angles in $[W^{V}(CN)_8]_{3-}$ units of **1**, **1hyd** and **2**

Complex	δ [deg]	φ [deg]
Ideal BTP-8	0; 21.8; 48.2; 48.2	14.1
Ideal SAPR-8	0; 0; 52.4; 52.4	24.5
Ideal DD-8	29.5; 29.5; 29.5; 29.5	0
$[W1(CN)_8]^{3-}$ in **1**-(*SS*)	15.7; 17.2; 42.0; 44.8;	21.6
$[W1(CN)_8]^{3-}$ in **1**-(*RR*)	14.9; 16.1; 41.1; 43.0;	21.0
$[W2(CN)_8]^{3-}$ in **1**-(*SS*)	7.6; 17.4; 44.5; 45.9;	26.4
$[W2(CN)_8]^{3-}$ in **1**-(*RR*)	8.1; 17.5; 45.3; 46.1;	26.6

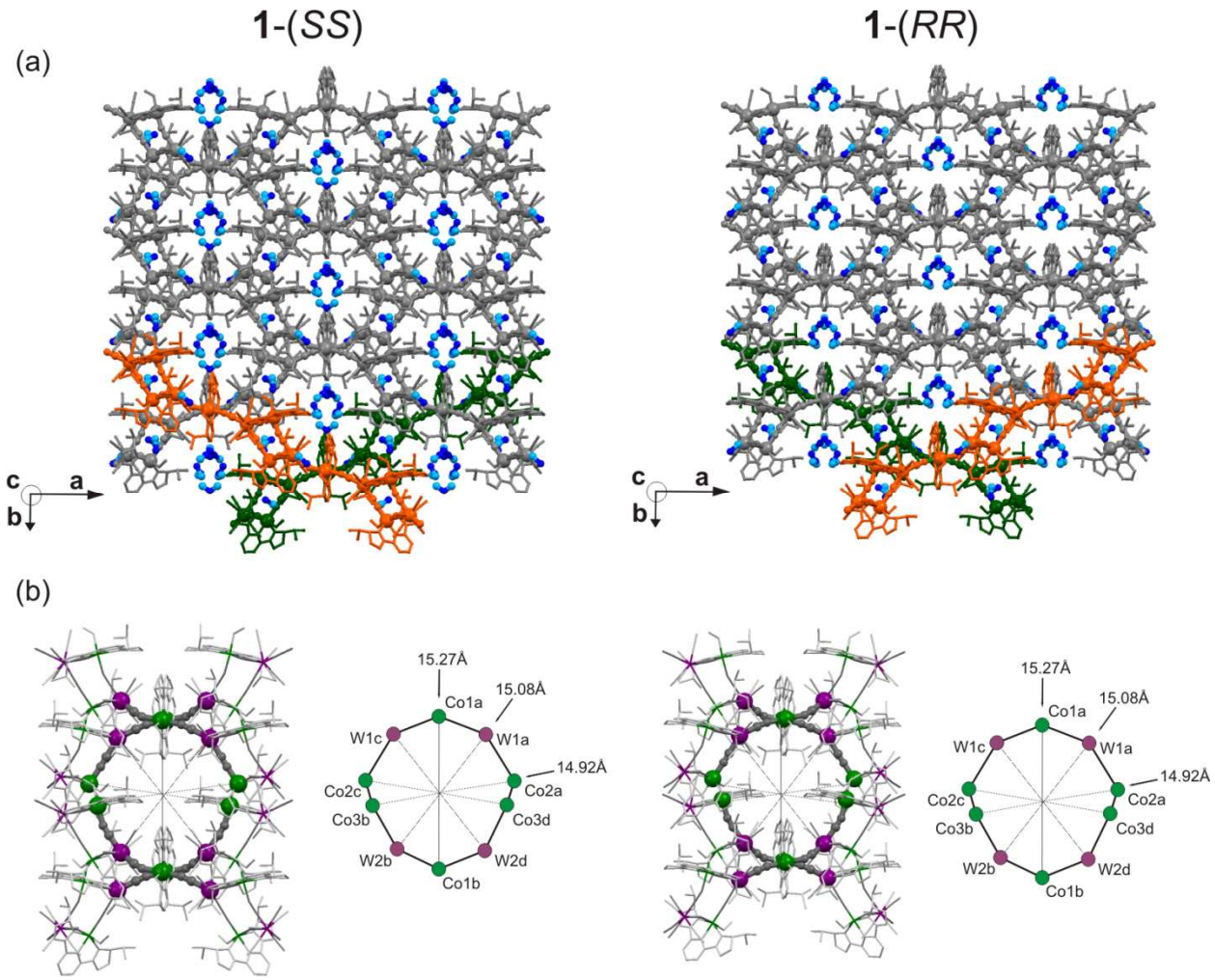

Figure S2. The crystal structure of **1**-(*SS*) and **1**-(*RR*): the view of microporous network with the enlargement of non-coordinated solvent (a) and the visualization of the shape and dimensions of single channel (b). Hydrogen atoms (a-b) and non-coordinated molecules (b) are omitted for clarity. The atom spheres of cyanide-bridged skeleton are enlarged. Colour code for (a): cyanides coordination skeleton – dark grey (two chosen chains: orange and green), N(methanol) – blue, O(methanol) – dark blue. Colour code for (b): W – purple, Co – green, O, C, N – grey.

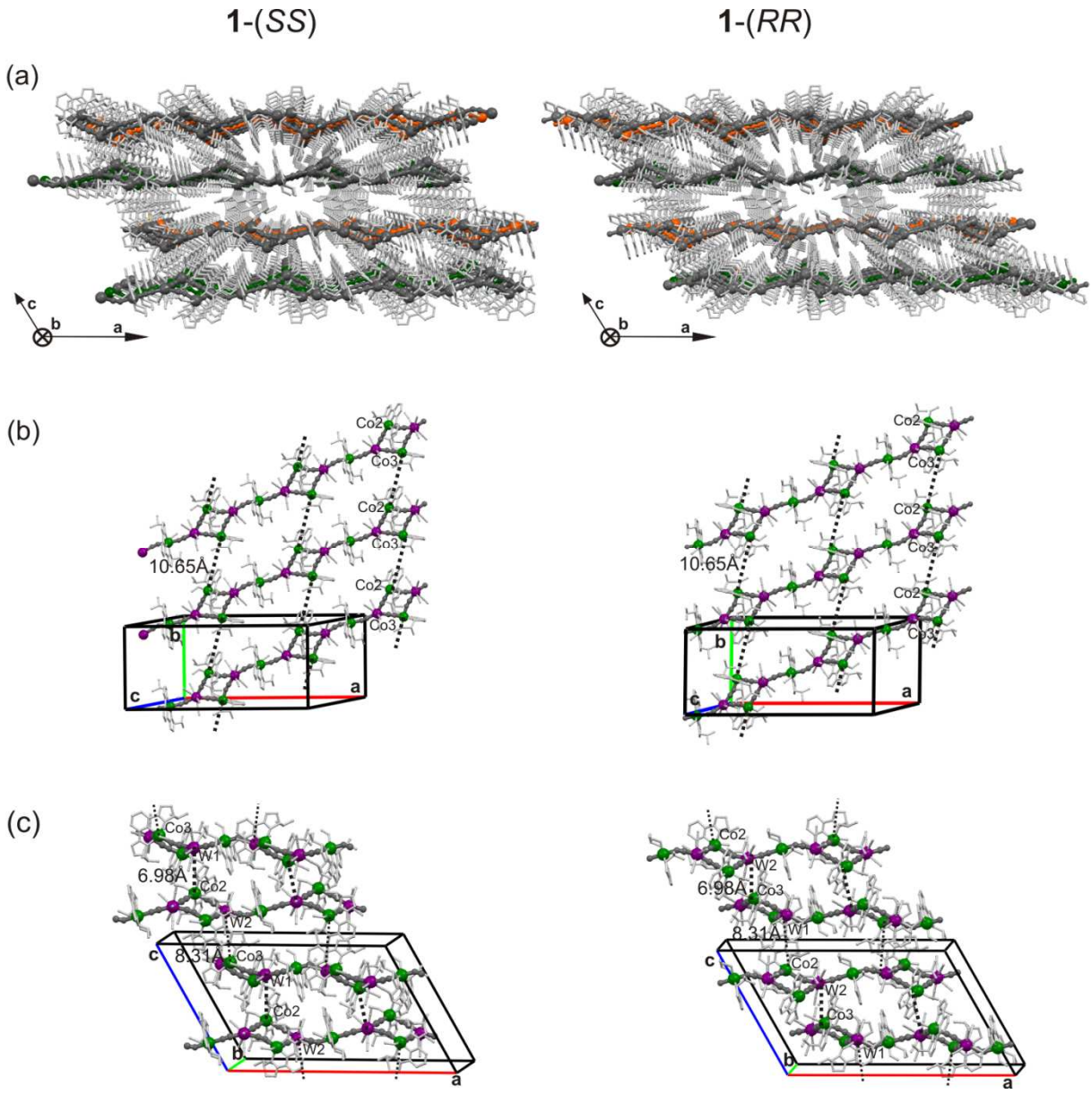

Figure S3. The crystal structure of **1**-(*SS*) and **1**-(*RR*): the view along *b* direction (a) and the closest interchain contacts within *ab* plane (b) and *ac* plane (c). Hydrogen atoms and non-coordinated molecules are omitted for clarity. Cyano-bridged skeletal atom spheres are enlarged. Colour code: W – grey (a) or purple (b,c), Co – grey (a) or green (b,c), O, C, N – grey.

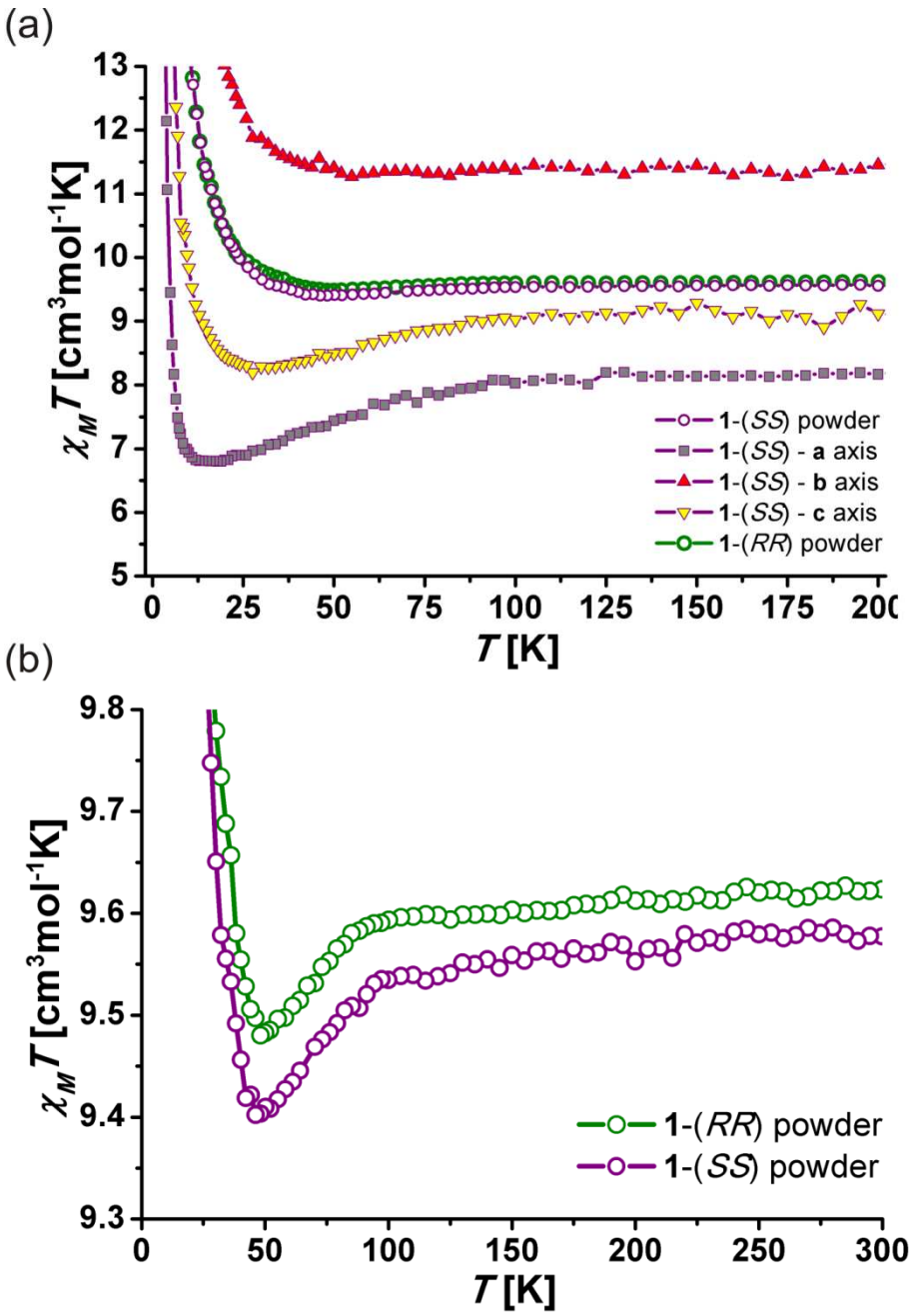

Figure S4. Magnetic properties of **1**-(*SS*) and **1**-(*RR*): (a) the enlargement of the minima in the $\chi_M T$ versus *T* plots for **1**-(*SS*) (powder sample and *a*, *b*, *c* axis of the single crystal) and **1**-(*RR*) (powder); (b) the closer enlargement of the $\chi_M T$ minima for powder samples.

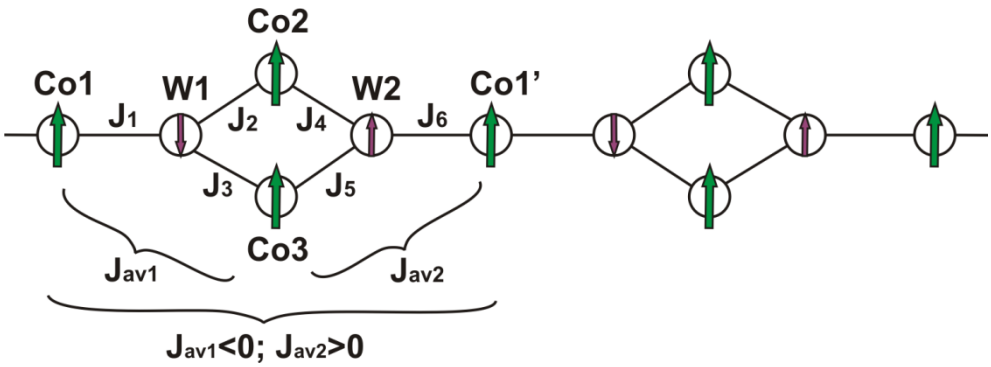

Figure S5. The possible spin arrangement in **1**-(*SS*) and **1**-(*RR*) explaining magnetic data (the case of $J_{av1}<0$ and $J_{av2}>0$).

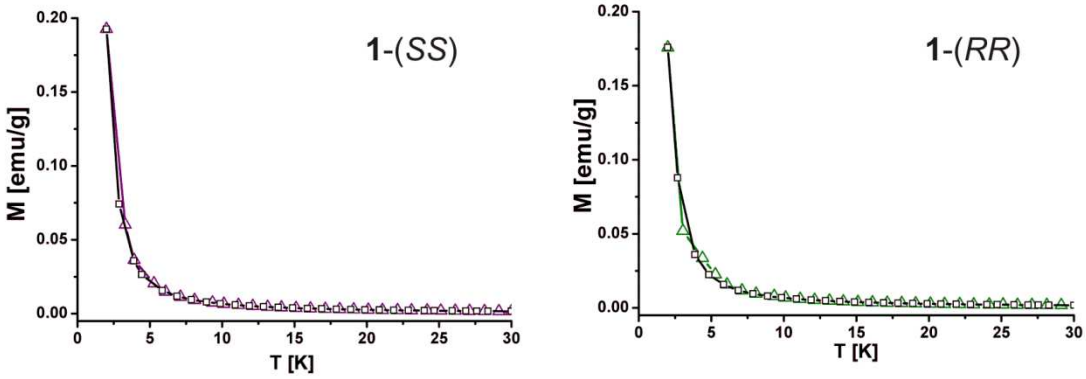

Figure S6. Zero-field-cooled magnetization (ZFCM, empty black symbols) and field-cooled magnetization (FCM, coloured symbols) at 10Oe in the 2-30K range for **1**-(*SS*) and **1**-(*RR*).

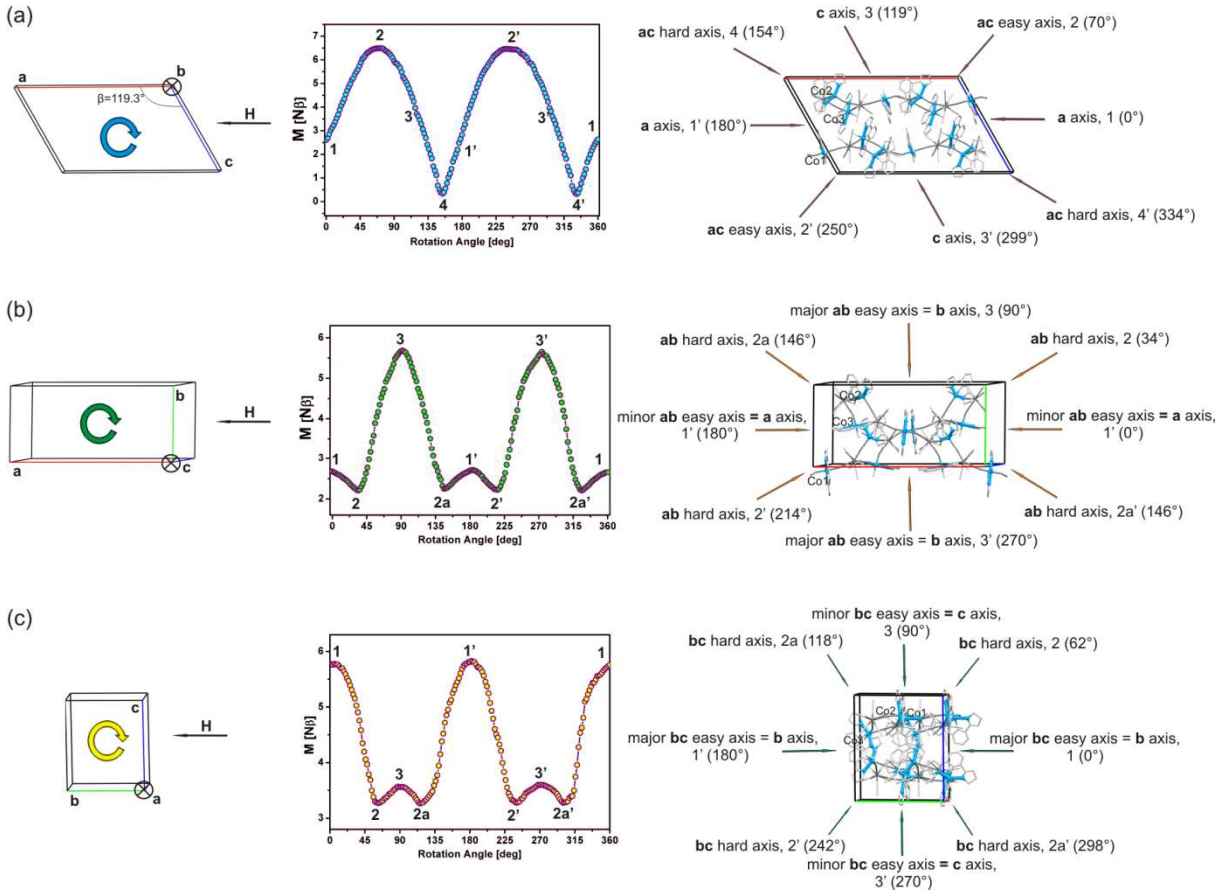

Figure S7. Magnetic properties of oriented crystal of **1**-(*SS*) – detailed analysis of rotation dependences of magnetization in *ac* (a), *ab* (b) and *bc* (c) plane: results of measurement (left) and the arrangement of magnetization axes in relation to the structure (right).

Comment:

The alignment of magnetization axes for *ac* plane (a) was discussed in the main text. The magnetic data for *ab* and *bc* plane shows more complicated scheme with two types of easy axes (b,c). For both cases the major one is parallel to *b* axis which can be mainly explained by the arrangement of Co1-N(oxazoline) linkages along this axis. Interestingly also the minor easy axes of magnetization are consistent with the crystallographic axes: *a* and *c*, respectively. That is connected with the fairly good alignment of Co3-N(oxazoline) in relation to *a* and Co2-N(oxazoline) bonds in relation to *c*. The hard axis within the *ab* plane was found 34° (or 146°) going from *a* to *b* and corresponds to the direction of molecular chains which is simultaneously closely perpendicular to all Co-N(oxazoline) linkages. Similar hard axes were observed in *bc* plane.

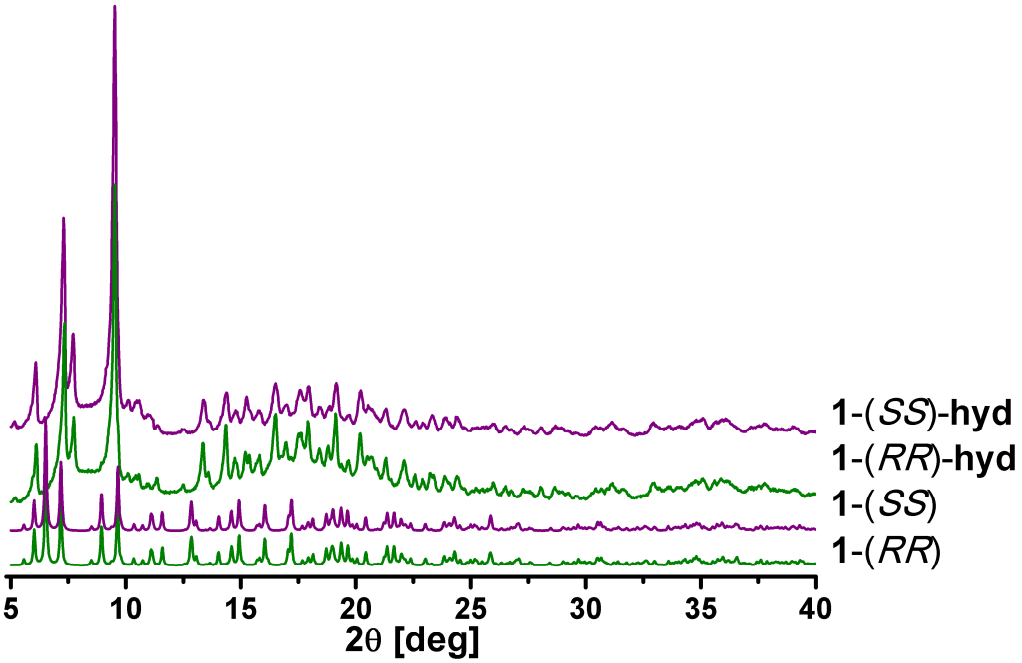

Figure S8. The comparative view of powder diffractograms for **1**-(*SS*), **1**-(*RR*) (simulated) and their hydrated forms obtained by drying on the air: **1**-(*SS*)-**hyd** and **1**-(*RR*)-**hyd**. Powder diffractograms for hydrated phases were measured on Rigaku RINT 2100 with Cu Kα radiation at 293(2)K.

References to Supporting Information

(S1) Zhong, Z. J.; Seino, H.; Mizobe, Y.; Hidai, M.; Fujishima, A.; Ohkoshi, S.; Hashimoto, K. *J. Am. Chem. Soc.* **2000**, *122*, 2952.

(S2) Song, Y.; Zhang, P.; Ren, X.-M.; Shen, X.-F.; Li, Y.-Z.; You, X.-Z. *J. Am. Chem. Soc.* **2002**, *127*, 3708.

(S3) Bonadio, F.; Gross, M.; Stoeckli-Evans, H.; Deucrtins, S. *Inorg. Chem.* **2002**, *41*, 7524.

(S4) Hilfiger, M. G.; Zhao, H.; Prosvirin, A.; Wernsdorfer, W.; Dunbar K. R. *Dalton Trans.* **2009**, *38*, 5155.

(S5) Jeong, H. L.; Houng, S. Y.; Jae, I. K.; Jung, H. Y.; Yang, N.; Eui, K. K.; Park, J.-G.; Chang, C. H. *Eur. J. Inorg. Chem.* **2008**, *22*, 3428.

(S6) Lim, H.; Yoon, J. H.; Kim, H. C.; Hong, C. S. *Angew. Chem. Int. Ed.* **2006**, *45*, 7424.

(S7) Podgajny, R.; Nitek, W.; Rams, M.; Sieklucka, B. *Cryst. Growth Des.* **2008**, *8*, 3817.

(S8) Podgajny, R.; Chorazy, S.; Nitek, W.; Rams, M.; Bałanda, M.; Sieklucka, B. *Cryst. Growth Des.* **2010**, *10*, 4693.

(S9) Li, D.; Zheng, L.; Zhang, Y.; Huang, J.; Gao, S.; Tang, W. *Inorg. Chem.* **2003**, *42*, 6123.

(S10) Samotus, A. *Pol. J. Chem.* **1973**, *47*, 653.

(S11) Sheldrick, G. M. *Acta Crystallogr.* **2008**, *A64*, 112.

(S12) Llunell, M.; Casanova, D.; Cirera, J.; Bofill, J.; Alemany, P.; Alvarez, S.; Pinsky, M.; Avnir, D., SHAPE v. 1.1b. Program for the Calculation of Continuous Shape Measures of Polygonal and Polyhedral Molecular Fragments, University of Barcelona: Barcelona, Spain, 2005.

(S13) Casanova, D.; Cirera, J.; Llunell, M.; Alemany, P.; Avnir, D.; Alvarez, S. *J. Am. Chem. Soc.* **2004**, *126*, 1755.

(S14) Alvarez, S.; Alemany, P.; Casanova, D.; Cirera, J.; Llunell, M.; Avnir, D. *Coord. Chem. Rev.* **2005**, *249*, 1693.